Distribution of the Angular Momenta, Level Spacings, and Neutron Widths of Al^{28}†*

CARL T. HIBDON
Argonne National Laboratory, Lemont, Illinois
(Received November 7, 1958)

The neutron total cross section from about 1 kev to 450 kev shows the presence of sixty-six peaks, seven of which are of the s-wave variety. Thirteen resonances are attributable to $J=0$, twenty-one to $J=1$, eighteen to $J=2$, ten to $J=3$, and three to $J=4$. This distribution is in agreement with the theoretical distribution for a value of $2c\tau\equiv 2\sigma^2=6$. The density of all levels for this energy interval is 146 Mev^{-1} and the average level spacing of the nucleons is 0.48 Mev. The neutron widths vary from 1 to 7 kev and the distribution of the reduced widths appears to agree with an exponential distribution and is also in fair agreement with the Porter-Thomas distribution. The level spacings also agree with an exponential distribution. As obtained from the reduced widths averaged over both values of J, the value of the strength function for $l=0$ is 0.05, averaged over all values of J for $l=1$ it is 0.49, and for $l=2$ it is too large in comparison with the p-wave strength function. The particularly low value of the cross section below 30 kev and the shape of the wings of the 35-kev resonance can be explained by a multiple-level computation of the interference of the s-wave levels. On the basis of the results of the present analyses, the levels are about equally divided between the odd and even values of l.

1. INTRODUCTION

VIRTUAL nuclear energy levels of nuclei can be located and studied by measuring the variation of the neutron total cross section as a function of neutron energy. With the resolution now achieved, it is possible to obtain sufficiently detailed information to study the level spacings, resonance parameters, strength functions, and the distribution in size of the neutron widths and of the angular momenta among the levels of the compound nucleus.

The present paper is concerned with measurements on Al^{27} from about 1 to 450 kev. Previous measurements indicated the presence of a number of resonances in the low-energy region.[1–3] It was shown later that these resonances were due to a manganese impurity.[4] Recent measurements at Columbia University and at Harwell[5] do not show any resonance structure from 1 ev up to 4 kev. One resonance, variously quoted at from 5.5 to 9 kev, does persist.[6–8]

The cross section of aluminum up to 800 kev was first measured by Seagondollar and Barschall[9] by use of neutrons with a large energy spread and with most points taken at intervals of approximately 10 kev. A dozen or so resonances were observed. Later measurements of the (n,γ) cross section by Henkel and Barschall[10] also showed a number of resonances up to 500 kev. Some of these capture resonances (notably near 40, 215, and 370 kev) coincide with resonances previously found by Seagondollar and Barschall[9] but others do not. From this, it was concluded that the transmission measurements missed a number of resonances that smaller neutron energy spreads currently in use could resolve and the resonances which were previously observed could be resolved better. The group at Duke University[11] has studied the resonance at 35 kev and near 90 kev but reported no measurements at higher energies.

2. EXPERIMENTAL METHOD

The experimental procedure and techniques are the same as were used previously and described in detail in the paper on Fe and Cr.[12] The counting equipment, however, has been modified further so that the 86 counters of Fig. 1 in reference 12 are replaced by a similar arrangement of 50 larger proportional counters in a longer cylinder of paraffin. Each neutron counter now in use has a diameter of 1.5 in. and an active length of 20 in. and is filled to a pressure of 45 cm Hg with boron trifluoride gas in which the boron is enriched to 96% B^{10}. Each group of 12 or 13 counters feeds into

† Work performed under the auspices of the U. S. Atomic Energy Commission.

* For the preliminary results of the measurements on Al^{28}, some results of analyses of its resonances, and the distribution of angular momenta among its nuclear levels, see C. T. Hibdon, Bull. Am. Phys. Soc. Ser. II, **2**, 232 and 354 (1957); **3**, 48 (1958).

[1] *Neutron Cross Sections*, compiled by D. J. Hughes and J. A. Harvey, Brookhaven National Laboratory Report BNL-325 (Superintendent of Documents, U. S. Government Printing Office, Washington, D. C., 1955); and Supplement No. 1, compiled by D. J. Hughes and R. B. Schwartz, 1957; and the second edition, compiled by D. J. Hughes and J. A. Harvey, 1958. These compilations will be referred to as BNL-325.

[2] Coster, Groendijk, and DeVries, Physica **14**, 1 (1948).

[3] Goldsmith, Ibser, and Feld, Revs. Modern Phys. **19**, 259 (1947).

[4] C. T. Hibdon and C. O. Muehlhause, Phys. Rev. **76**, 100 (1949).

[5] A. W. Merrison and E. R. Wiblin, Proc. Roy. Soc. (London) **A215**, 278 (1952). The measurements at Columbia University apparently have not been published but the results are shown in BNL-325, Supplement No. 1 (reference 1).

[6] Lichtenberger, Nobles, Monk, Kubitschek, and Dancoff, Phys. Rev. **72**, 164(A) (1947); L. E. Beghian and H. H. Halban, Nature **163**, 366 (1949).

[7] Roher, Newson, Gibbons, and Cap, Phys. Rev. **95**, 302(A) (1954).

[8] Good, Neiler, and Gibbons, Phys. Rev. **109**, 926 (1958).

[9] L. W. Seagondollar and H. H. Barschall, Phys. Rev. **72**, 439 (1947).

[10] R. L. Henkel and H. H. Barschall, Phys. Rev. **80**, 145 (1950).

[11] Crutchfield, Haeberli, and Newson, Bull. Am. Phys. Soc. Ser. II, **2**, 33 (1957).

[12] C. T. Hibdon, Phys. Rev. **108**, 414 (1957).

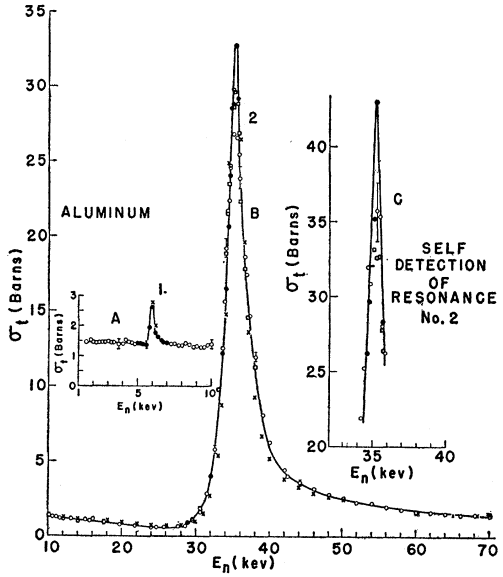

FIG. 1. Neutron total cross section of aluminum up to 70 kev. (*A*) Solid circles in the region of the 6-kev peak show data obtained with a neutron energy spread of about 400 ev. (*B*) Peak heights of resonance No. 2 attained by neutron energy spreads of 450 ev (squares), 400 ev (open circles), and 325 ev (solid circles). (*C*) Data obtained by self-detection. Neutron energy spreads are the same as for (*B*).

one of four amplifiers. This modification improves the ratio of counts to background so that data can be collected about twice as fast.

In addition to the vertical slits mentioned in reference 12, a horizontal slit 0.125 in. wide has also been placed a few inches before the entrance to the electrostatic analyzer, a second similar slit just before the vertical exit slits, and a third one just ahead of the lithium target assembly. These slits permit a viewing of the proton beam for alignment purposes and allow very little vertical movement of the proton beam on the lithium target.

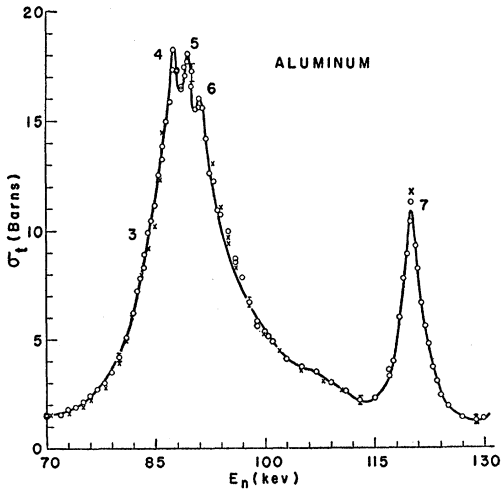

FIG. 2. Neutron total cross section of aluminum from 70 to 130 kev. The point marked by a cross above resonance No. 7 was obtained by self-detection. The crosses from 70 to 114 kev represent points computed as explained in the text.

Samples of aluminum purporting to be of 99.9% purity were used for the measurements. Up to 30 kev, the data do not show any reasonable structure to indicate the presence of impurities. The small peak at 6 kev alone cannot be attributed to any known isotope that might be present as an impurity. A further check was made by a spectrochemical analysis in which the only detected impurities were 0.05% Fe and 0.05% Si.

The first measurements were made up to 415 kev by use of neutron energy spreads ranging from 400 to 700 ev. During various later runs these measurements were repeated and extended up to 450 kev by use of neutron energy spreads ranging between 300 and 400 ev. A number of the resonances were also studied by the self-detection technique.[12] The neutron energy spreads were estimated by the method outlined in reference 12.

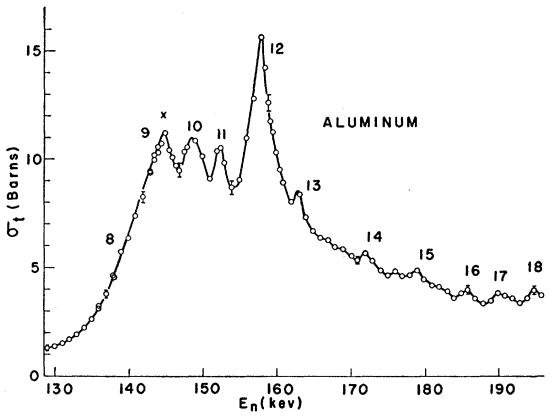

FIG. 3. Neutron total cross section of aluminum from 130 to 196 kev. The point marked by a cross above resonance No. 9 was obtained by self-detection.

At the higher energies it is expected that the energy spreads become somewhat larger than those quoted.

3. EXPERIMENTAL RESULTS

Figures 1 through 7 show the observed neutron total cross section of aluminum as a function of neutron energy from about 1 to 450 kev. All of the dozen or so levels previously observed by Seagondollar and Barschall[9] and by Henkel and Barschall[10] were observed along with many additional ones. Variations in the cross section show a complicated level structure for the nuclide Al^{28}. Most of the peaks do not appear to be *s*-wave resonances ($l=0$). These are identifiable by two distinguishable characteristics: the presence of low minima on the low-energy sides of the resonances and an asymmetrical shape. Moreover, adjacent pairs of reasonably well separated resonances of this type are expected to show marked interference minima between them. Actually, indications of these expectable minima are found with only a relatively small number of

resonances. For the others l must be greater than zero (p and d wave, etc.) because of the observable features of the data, so one expects a profusion of p- and d-wave resonances. The various peak heights seem to indicate the presence of an assortment of values of J.

Only a few of the resonances are sufficiently well isolated to obtain values of J and Γ directly, and even these can be analyzed better by taking account of the

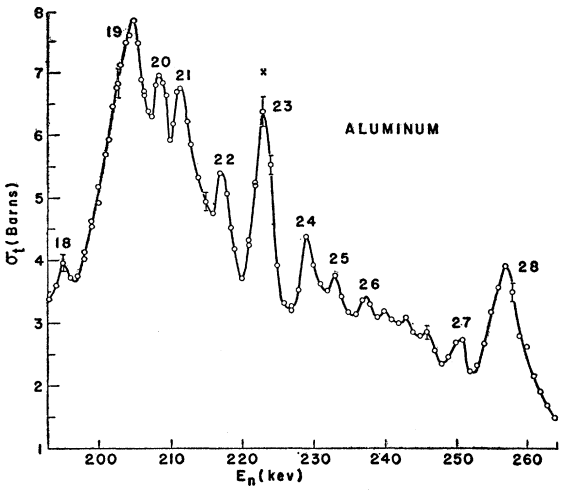

FIG. 4. Neutron total cross section of aluminum from 193 to 265 kev. The point marked by a cross above resonance No. 23 was obtained by self-detection.

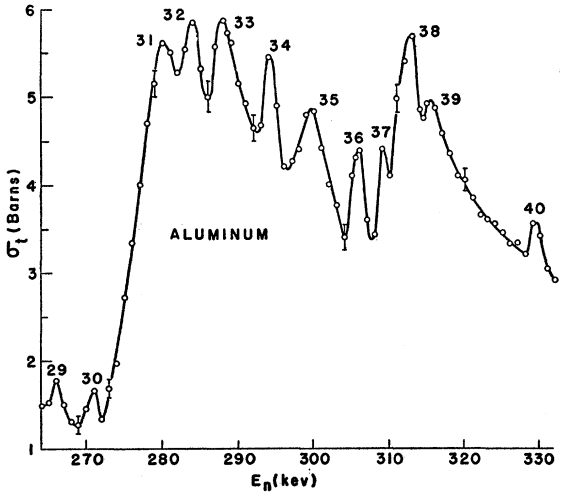

FIG. 5. Neutron total cross section of aluminum from 265 to 330 kev.

interfering wings of other resonances. Most of the resonances occur in overlapping clusters and the interfering wings must be considered. It proves possible to do this and to make fairly unamiguous analyses of these clusters, principally because of the very limited number of possible values for the peak cross sections.

The reactions $Al^{27}(n,n')Al^{27}$ and $Al^{27}(n,p)Si^{27}$ will not contribute to the cross section in the present measure-

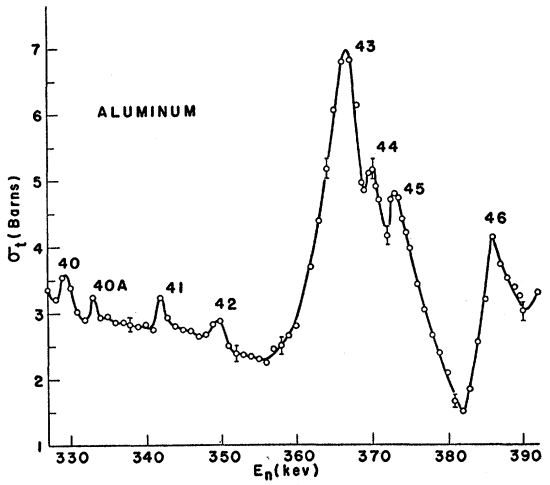

FIG. 6. Neutron total cross section of aluminum from 328 to 393 kev.

ments because their thresholds are at higher energies.[13,14] Measurements by Henkel and Barschall[10] showed that radiative capture contributes to some but not all of the resonances of aluminum. They estimated the neutron absorption widths of the resonances to be no more than 15 ev. In the present measurements the total width of all observed levels, except the level at 6 kev, ranges from 1 to 7 kev. Thus one can ignore the capture and treat the resonances of aluminum in this energy region as simple elastic-scattering resonances.

The neutron beam contains a second group of low-energy neutrons that arises from the formation of the residual nucleus Be^7 in the 430-kev excited state. Because of this the various resonances at low energies may produce small peaks at higher energies.[12] When the main group of neutrons has an energy of 333 kev, the low-energy component has an energy of 35 kev. There-

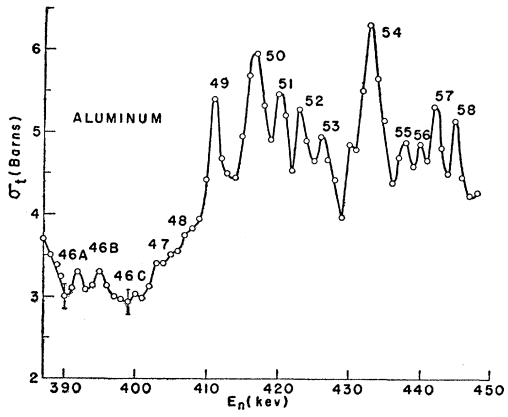

FIG. 7. Neutron total cross section of aluminum from 387 to 450 kev.

[13] P. M. Endt and C. M. Braams, Revs. Modern Phys. **29**, 683 (1957).

[14] E. Bretscher and D. H. Wilkinson, Proc. Cambridge Phil. Soc. **45**, 141 (1949).

fore, the 35-kev resonance re-appears as a spurious peak (No. 40A in Fig. 6) at 333 kev, which thus can be accounted for by assuming that about 3% of the beam of neutrons is in the low-energy group. Similarly, if above 390 kev the low-energy group constitutes 4 to 5% of the beam, the irregularities there (small peaks 46A, 46B, and 46C in Fig. 7) may be spurious reflections of the group of resonances (No. 3 through No. 6) near 90 kev. The small peak just below resonance No. 54 can be attributed to resonance No. 7 at 120 kev if the beam of neutrons exciting it consists of about 8% of the low-energy group of neutrons. These small peaks are, therefore, not considered to represent levels of Al^{28} and are excluded from the analyses. The abundances of low-energy neutrons found here for the three different energies appear to be in agreement with previous measurements. These abundances and references to the original papers are collected on page 420 in reference 12.

4. IDENTIFICATION OF THE RESONANCE LEVELS

(A) Preliminary Considerations

The analyses of the resonances are based on the multiple-level neutron scattering dispersion formula[15] which, except for levels whose widths are larger than or about equal to the level spacing, is given in the form

$$\sigma_s=4\pi\lambda\!\!\!^{-2}\sum_l\sum_J g_{J,l}\left|\sum_r\frac{\frac{1}{2}\Gamma_r}{E-E_r+\frac{1}{2}i\Gamma_r}+e^{i\delta_l}\sin\delta_l\right|^2. \quad (1)$$

The subscript r designates a particular level of the J,l type. For a group of levels having the same values of J and l, Eq. (1) expands into the form

$$\sigma_s=\sigma_p+\pi\lambda\!\!\!^{-2}g_{J,l}\left\{\sum_r\frac{\Gamma_r^2(1-2\sin^2\delta_l)+4\Gamma_r(E-E_r)\sin\delta_l\cos\delta_l}{(E-E_r)^2+\frac{1}{4}\Gamma_r^2}+\sum_r\sum_{(s\neq r)}\sum_s\frac{2\Gamma_r\Gamma_s}{[(E-E_r)^2+\frac{1}{4}\Gamma_r^2][(E-E_s)^2+\frac{1}{4}\Gamma_s^2]}[\tfrac{1}{4}\Gamma_r\Gamma_s+(E-E_r)(E-E_s)]\right\}. \quad (2)$$

Each term of the first summation inside the curly braces is identical with the single-level expression and represents the contribution of a single resonance and its interference with the potential scattering. There are, then, as many single-level terms as there are resonances. The second summation represents the mutual interference of the different pairs of resonances and there is a term for each possible pair. The potential scattering is given by $\sigma_p=\sum_l(2l+1)4\pi\lambda\!\!\!^{-2}\sin^2\delta_l$. For a single isolated level, Eq. (1) or (2) reduces to the familiar form known as the Breit-Wigner single-level dispersion formula:

$$\sigma_s=\sigma_p+\pi\lambda\!\!\!^{-2}g_{J,l}\frac{\Gamma^2(1-2\sin^2\delta_l)+4\Gamma(E-E_r)\sin\delta_l\cos\delta_l}{(E-E_r)^2+\frac{1}{4}\Gamma^2}. \quad (3)$$

The symbols in these formulas have their customary significance.[12] Possible values of J are computed by the method of Blatt and Weisskopf.[16] by defining $\phi=\theta+\delta_l$, where $\tan\theta=(E-E_r)/(\frac{1}{2}\Gamma)$, Eq. (3) reduces to the form

$$\sigma_s=\sigma_p+4\pi\lambda\!\!\!^{-2}g_{J,l}(\cos^2\phi-\sin^2\delta_l), \quad (4)$$

which for a maximum reduces to

$$\sigma_{\max}=4\pi\lambda\!\!\!^{-2}[g_{J,l}\cos^2\delta_l+\textstyle\sum_l(2l+1)\sin^2\delta_l]. \quad (5)$$

Equation (5) is then used for the purpose of computing the possible single-level peak heights of resonances for the various values of J and l. The minimum of a resonance is then given by the equation

$$\sigma_{\min}=\sigma_p-4\pi\lambda\!\!\!^{-2}g_{J,l}\sin^2\delta_l, \quad (6)$$

which is very nearly $(1-g)\sigma_p$ for $l=0$ because contributions from other values of l are negligible.

The number of compound levels that can be formed depends on the number of possible values of J and parity. Aluminum has only one isotope, Al^{27}; hence all observed resonances are levels of the compound nucleus Al^{28}. The nuclear spin[13,17] of Al^{27} is $I=\frac{5}{2}$ and the parity of the ground state is listed as even by King[18] and by Endt and Braams.[13] If the neutrons involved in the interaction are s-wave neutrons ($l=0$), the levels of the compound nucleus have a possible J of 2 or 3 and even parity; if p-wave ($l=1$), the values of J are either 1, 2, 3, or 4 and the levels have odd parity; and if d wave ($l=2$), the values of J are 0, 1, 2, 3, 4, or 5 and the levels have even parity. Hence, for $l\leqslant 2$, one may possibly see any of ten types of resonances differing in J or parity.

The observed width of the small peak (No. 1 in Fig. 1) is not distinguishably different from the neutron energy spread of 400 ev used for its measurement. Therefore, the level must be very narrow. On several different occasions the data indicated high points in this region. During two different runs the region was investigated by closely spaced points. This small peak

[15] The multiple-level formula in this or a similar form has been used by various experimenters for a number of years. See, for example, H. A. Bethe, Revs. Modern Phys. **9**, 69 (1957); Harris, Hibdon, and Muehlhause, Phys. Rev. **80**, 1014 (1950); Feshbach, Porter, and Weisskopf, Phys. Rev. **96**, 448 (1954); J. A. Moore, Phys. Rev. **109**, 417 (1958), Eqs. (10) and (11).

[16] J. M. Blatt and V. F. Weisskopf, *Theoretical Nuclear Physics* (John Wiley and Sons, Inc., New York, 1952), p. 426.

[17] J. E. Mack, Revs. Modern Phys. **22**, 64 (1950).

[18] R. W. King, Revs. Modern Phys. **26**, 327 (1954).

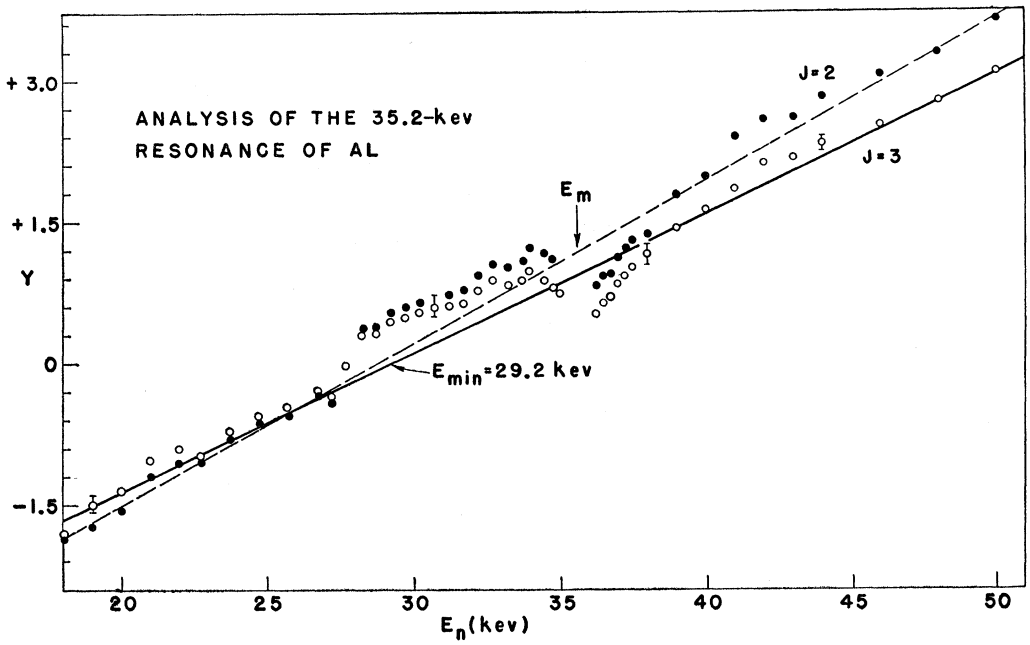

FIG. 8. Analysis of the 35.2-kev resonance of aluminum. The plot is shown for both $J=2$ (solid circles) and $J=3$ (open circles). See text and reference 12 for a description of the method and the definition of the complicated quantity Y.

was observed both times at 6 kev. Other experimenters have observed it also.[7,8]

(B) Analysis of the 35-kev Resonance

Resonance No. 2, whose peak is at 35.2 kev, clearly shows a pronounced minimum on the low-energy side and the asymmetrical shape characteristic of an s-wave resonance. A number of measurements were made in the region of this resonance in order to distinguish between the two possible values of $J=2$ and 3 corresponding to peak heights of 34.5 and 47 barns, respectively. Three different thicknesses of lithium targets were used during the latest measurements. Figure 1 shows the results for all three thicknesses and also the self-detection measurements for the same neutron energy spreads. The highest peak obtained by the thinnest target was 32.7 ± 2 barns and by self-detection by the same target a value of 43.7 ± 6 barns. Therefore, J is taken to be 3. To obtain the width of this resonance, it was analyzed by the method used by Hibdon[12] to analyze isolated s-wave resonances. This method, which uses a larger fraction of the points than do former methods, is described in detail in reference 12 and is based on the single-level formula, Eq. (3). Briefly, the method consists of arranging the equation in such a form that a plot of a quantity Y *vs* E over the region of the resonance is a straight line for a perfectly resolved, completely isolated resonance. This is done by expressing the parameters E_r, Γ, and δ in terms of their values for which σ_s has its maximum value. Then the potential scattering can be obtained from the slope of the straight line and the width from the ordinate of the line at the energy for which the scattering is a maximum. Figure 8 shows such a plot for each value of J and it is obvious that this plot makes no selection between the two values of J. The line for $J=3$ yields a value of $\Gamma=1.7$ kev and a value of 1.07 barns for $4\pi\lambda^2(7/12)\sin^2\delta_0$, that part of the apparent potential-scattering cross section corresponding to $J=3$. The value of the cross section at the minimum is 0.5 barn and corresponds to $4\pi\lambda^2(5/12)\times\sin^2\delta_0$, the apparent contribution to the potential scattering for $J=2$. Since these two contributions are in a ratio of 2.1 to 1 instead of the theoretical value of 7 to 5, it is clear that the effective value of δ_0 is different for the two values of J. These different apparent values for the potential scattering presumably are to be accounted for by different interference contributions from remote resonances of the two types. Later in this paper the low value of the potential scattering determined here, the shape of the lower parts of the wings of this resonance, and the deviation of the points in Fig. 8 from the straight line will be accounted for by including the wings of all contributing s-wave resonances and their mutual interference.

If resonance No. 2 were attributable to a value of $J=2$, one obtains a width of 2.2 kev and a value of 1.0 barn for $4\pi\lambda^2(5/12)\sin^2\delta_0$, the apparent contribution to the potential scattering for $J=2$. Then in this case the value of 0.5 barn at the minimum would be interpreted as the contribution for $J=3$. The ratio is then 2 to 1 rather than 5 to 7 as it should be for hard-sphere scattering.

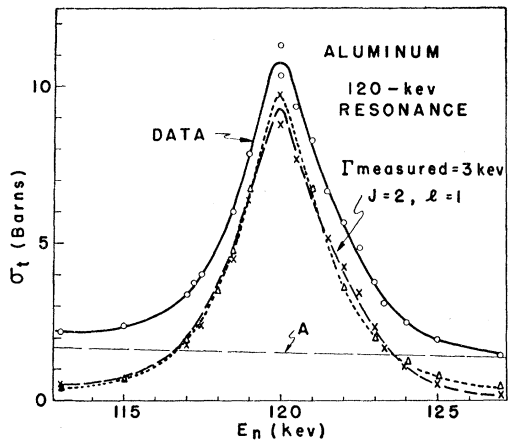

FIG. 9. Analysis of the 120-kev resonance. Points shown by crosses represent the resonance scattering after the wings (A) of other resonances have been subtracted from the data. The triangles represent points obtained by the single-level formula for $J=2$, $\Gamma=3$ kev and $l=1$.

(C) Analysis of the 120- and 257-kev Resonances

Two other resonances, No. 7 located at 120 kev and No. 28 at 257 kev, can be fairly well analyzed directly by estimating the backgrounds upon which they sit and obtaining the resonance scattering by subtracting this background from the data. Because of their apparent symmetrical shapes and the absence of pronounced minima in their low-energy wings, one can be reasonably sure that they are not s-wave resonances. The measured peak height of the 120-kev resonance is 11.3 barns (including the potential scattering) and the height by self-detection is 11.7 barns. These are to be compared with possible values of 12 and 16 barns for $J=2$ and 3, respectively. Use of smaller neutron energy spreads would not be expected to resolve a resonance of this apparent width to any appreciably higher peak value. Therefore it is considered well resolved and J has a value of 2. By a direct examination, one can see that the width of this resonance is very nearly 3 kev. This is confirmed by subtracting off the apparent background upon which it sits and making a single-level plot for this width by use of Eq. (3) and also using $J=2$ and $l=1$. A slightly better agreement with the single-level plot occurs for the low-energy wing if the combined wings of the s-wave resonances Nos. 4, 6 and 9 obtained by multiple-level computations are used as the background, the higher energy wing being in very good agreement and unchanged by this background. This background is shown in Fig. 9 by curve A. The result of subtracting curve A from the experimental curve is shown in Fig. 9 by the curve with points indicated by crosses. The curve with points indicated by triangles is the single-level plot for $J=2$, $\Gamma=3$ kev, and $l=1$.

Because of the width of the 257-kev resonance (No. 28), it is considered well resolved. The best estimate of the background upon which this resonance sits (although less accurate than for No. 7, principally because of resonance No. 27) is sufficient to obtain the value of J and a fair estimate of the width. A better analysis can be obtained by taking the background to be the sum of the wings of the nearby s-wave resonances, principally No. 31. The combined effect of the wings of these resonances is shown by curve A in Fig. 10. This curve which was obtained by the multiple-level formula, Eq. (2), was subtracted from the data to obtain the residual curve B. The peak height of the resonance is then 2.65 barns, compared with possible heights of 2.8 and 4.5 barns for $J=1$ and 2, respectively. The value of J is then taken to be 1. Curve C is the single-level plot obtained by using $J=1$, $\Gamma=5$ kev and $l=1$. By subtracting curve C from B, one obtains the adjacent peaks Nos. 27 and 29, shown as the two parts of curve D.

(D) Analysis of the Resonances in the Region from 355 to 390 kev

Except for a few small peaks, all of the other resonances tend to occur in clusters. It has been found possible to analyze these clusters by a "peeling-off" process. To give the detailed analyses of every group of resonances represented here would involve voluminous discussion and a prohibitive number of figures. A detailed analysis of one of the simpler groups is, therefore, given here. This is followed by a short description of the salient features necessary for the analysis of the other groups with the figures omitted. The successive steps for this type of analysis are illustrated in Figs. 11 and 12 for one of the less complicated groups. Because of the distinctly asymmetrical shape and the pronounced minimum on the low-energy side, resonance No. 46 in Fig. 11 is taken to be an s-wave resonance. Its peak height is very near the theoretical value for $J=2$. By trial and error it was found that a width of $\Gamma=4$ kev gives a reasonable fit to the data if

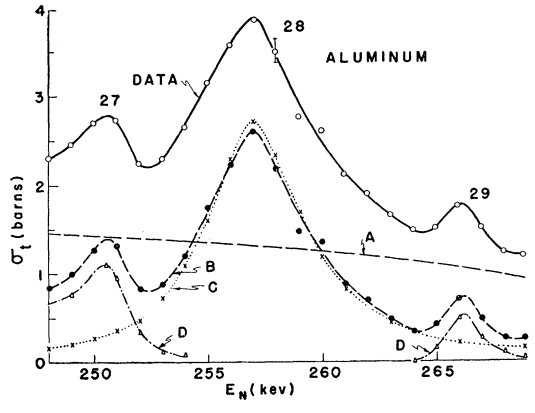

FIG. 10. Analysis of the 257-kev resonance. Points represented by solid circles show the resonance scattering after subtracting the wings (A) of other large resonances from the data. The crosses represent points obtained from the single-level formula for $J=1$, $\Gamma=5$ kev and $l=1$. The two parts of curve D are the results obtained by subtracting curve C from curve B.

one assumes the potential scattering in this region to be 2 barns, the value indicated by the low-energy wings of resonances Nos. 43 and 46. In Fig. 11, points computed by use of the single-level dispersion formula, Eq. (3), are shown in curve A, which is subtracted from the data to obtain curve B. Curve B is then transferred to Fig. 12, the points being shown as open circles. The symmetrical resonance No. 43 is a close fit to points obtained by using the parameters $\Gamma=5$ kev, $J=4$ and $l=1$ in the single-level formula as shown by the dotted curve with points marked by triangles. The high-energy wing of No. 43 is subtracted from curve B to obtain curve C, which is then transferred to the insert of Fig. 12 where it is shown by open circles. The peak height of resonance No. 45 is 2.5 brans, compared with theoretical heights of 1.9 and 3.1 barns for $J=1$ and 2, respectively. Hence a value of $J=2$ appears to be the correct one. Points obtained by the single-level formula by use of $\Gamma=3.5$ kev, $J=2$ and $l=1$ are shown as solid circles and appear to be a best fit to resonance No. 45. The difference between the low-energy wing and curve C shows the small peak No. 44 with points represented by triangles. The height of this peak is near 1.3 barns compared with values of 0.6 and 1.8 barns for $J=0$ and 1, respectively. Undoubtedly $J=1$ is the correct value. The curve with its points represented by crosses was computed from the single-level formula for $\Gamma=2$ kev, $J=1$ and $l=1$ and differs little from the same curve for $l=2$. It will be shown later that $l=2$ is probably the better choice.

(E) Analysis of the Resonances in the Region from 60 to 110 kev

To obtain a satisfactory analysis of this group (Figs. 1 and 2) it is necessary to proceed more or less by trial

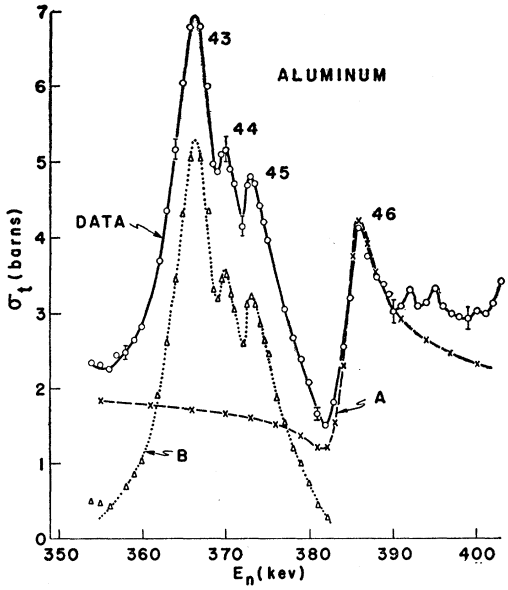

FIG. 11. Analysis of the resonances in the region from 355 to 390 kev. See the text for a description of the method.

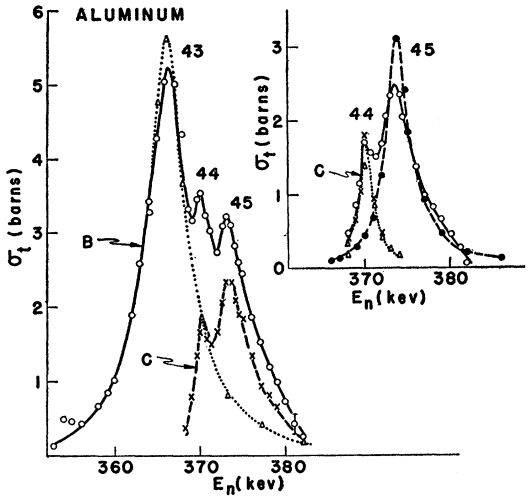

FIG. 12. Analysis of the 366-kev resonance No. 43. The insert shows the analyses of resonances Nos. 44 and 45 at 370 and 374 kev, respectively. See the text for the results.

and error until a reasonably satisfactory analysis has been obtained. The following noticeable features are useful aids in the analysis of this group: (*a*) Three peaks (Nos. 4, 5, and 6) are clearly present and a fourth one (No. 3) near 84 kev is indicated by a slight bulge. (*b*) The fact that the cross section between any pair of peaks does not go to a lower value than it does indicates that the width of each peak must be at least as large as 2 kev. On the other hand, the observed degree to which these peaks are resolved shows that the widths are unlikely to be greater than about 5 kev. (*c*) The theoretical value of the potential scattering cross section in this region [given by $\sum_l(2l+1)4\pi\lambda\!\!\!^{-2}\sin^2\delta_l$, where δ_l is computed using $R=R_0A^{\frac{1}{3}}$ and $R_0=0.14\times10^{-12}$ cm] is 2.17 barns. The value of the potential scattering indicated by the analysis of the 35-kev resonance is 1.57 barns and there is no reason to expect a lower value in this region. (*d*) The very low value of 1.4 barns near 70 kev is, therefore, indicative of s-wave interference. The absence of a deeper minimum closer to one of the peaks suggests that the indicated resonance near 84 kev is contributing more to the cross section than appears at a first glance. (*e*) The asymmetrical shape of this group of resonances, with high values of the cross section on the high-energy side, is also indicative of the presence of s-wave scattering.

For s-wave scattering, the possible values of J are 2 and 3. No pair of adjacent resonances in the group can have $l=0$ and the same J since there is no indication of any deep interference minimum such as this would produce. There are then the following provisional possibilities for s-wave scattering: (*a*) There is only one s-wave resonance for which $J=2$ or 3. (*b*) There are two present with $J=3$ and 2, respectively. (*c*) There are three present with J values of either 3–2–3 or 2–3–2 for resonances Nos. 4, 5, and 6. Of the two possibilities listed in (*c*), the first is ruled out by the low observed

TABLE I. Summary of the levels of Al^{28} derived from neutron reactions with Al^{27}. The parameters J, Γ, and l are probable values obtained as a best fit to the data. See text for the distinction between $l=1$ and 2.

No.	E_r (kev)	J	Γ (kev)	l	No.	E_r (kev)	J	Γ (kev)	l
1	6	...	...	...	27	250.5	0	3	2
2	35	3	1.7	0	28	257	1	5	1
3	84	1	5	1	29	266	0	1.5	2
4	86.6	3	2.4	0	30	271	0	1.5	2
5	89	1	2	1	31	278	3	5	0
6	91.5	2	4	0	32	284	1	2.5	1
7	120	2	3	1	33	288	2	3	1
8	140	1	5	1	33A	292	1	1.5	2
9	143.3	3	3.5	0	34	294.5	2	2	1
10	149	2	3	1	35	300	2	4	1
11	152	1	3	1	36	305.5	2	2	1
12	158	4	4	1	37	309	2	2	1
13	163	1	2	1	38	311.8	3	4	0
13A	166.5	1	1.8	1	39	316.5	0	1.5	2
13B	169	0	2.5	2	40	329.5	0	1.5	2
14	172	1	2	1	41	342	0	1.5	2
14A	175.5	0	3	2	42	349.5	0	1.5	2
15	179	1	2	1	43	366	4	5	1
15A	182	0	2	2	44	370	1	2	2
16	185.5	0	2.5	2	45	374	2	3.5	1
17	190.5	0	3	2	46	384.8	2	4	0
18	195	0	2	2	47	404.5	1	2	2
19	204	2	7	1	48	407.5	1	2	2
20	209	1	1.8	1	49	411	3	2	2
21	212	2	2	1	50	416.5	3	3.5	1
22	217	2	1.5	1	51	420.5	3	1.5	2
23	223	2	3	1	52	423	2	1.5	2
24	229	1	2	1	53	426	2	2.5	2
25	233	1	2	1	54	433	4	4	1
26	237.5	1	1.5	1	55	437.5	2	1.5	2
26A	240.5	1	1.5	1	56	439.5	2	1.4	2
26B	243	1	1	2	57	442	3	1.5	2
26C	245.5	1	1.5	1	58	445	3	1.5	2

peak height of resonance No. 6. For either of these assignments, the constructive interference of the two resonances of the same J would be expected to cause the cross section on the high-energy side of the group to exceed the observed value and to produce a minimum close to the low-energy side of the resonance of lower energy. This minimum, however, would be masked by the presence of No. 3 near 84 kev. Since there seems to be no straightforward method of reaching unambiguous conclusions, one can only test various trial assumptions by comparing their consequences with experiment. The set of parameters for the various resonances shown in Table I are the only ones that were found to yield reasonable results. However, in view of the numerous parameters involved, it cannot be claimed that this is necessarily the unique solution.

There are appreciable mutual interference effects among Nos. 2, 4, and 9 ($l=0$, $J=3$) and also between Nos. 3 and 5 ($l=1$, $J=1$). No way was found to account for the peculiar shape of the low-energy wing of No. 3 unless its mutual interference with No. 5 was included. Finally the computed contributions of all resonances from No. 2 to No. 9 inclusive, including the mutual interference effects, account very closely for the cross section of the wings from 60 to 114 kev. This is shown in Figs. 1 and 2 where computed points are represented by crosses.

(F) Analysis of the Resonances in the Region from 130 to 195 kev

The analysis of this group (Fig. 3) up through resonance No. 12 is very similar to the previous group from 60 to 110 kev. (The small peaks above No. 12 are reserved for later consideration.) The following observations provide clues for the analysis: (*a*) Four peaks, Nos. 9, 10, 11, and 12, are clearly present and a fifth, No. 8 is indicated near 140 kev. (*b*) A common value of J and l does not appear possible for any two adjacent resonances because of the absence of any deep minimum which would indicate the mutual interference of such a pair. (*c*) Resonance No. 12 certainly has a higher value of J than any other peak and it obviously has a width of about 4 to 5 kev, making allowances for the wings of adjacent peaks. The shape of its low-energy wing does not indicate *s*-wave scattering and also its peak height is several barns above either possible peak height for *s*-wave scattering. (*d*) The very low value of 1.3 barns for the cross section at 129 kev is indicative of *s*-wave scattering by at least one resonance in this group. The absence of a deeper minimum closer to one of the peaks suggests that resonance No. 8 is contributing strongly to the cross section. (*e*) Because of the various peak heights and the absence of deep minima, only one of Nos. 9, 10, or 11 can be due to *s*-wave scattering.

To obtain a successful analysis it was first necessary to locate the *s*-wave resonance and its parameters. It soon was found that No. 9 would lead to best results.

The observed height of this peak (11.2 barns, resolved to 12 barns by self-detection, compared with possible heights of 9.4 and 12.3 barns for $J=2$ and 3, respectively) indicates a value of $J=3$. By trial and error it was found by Eq. (3) that the width should be between 3 and 4 kev. By including the mutual interference with Nos. 4 and 31 ($J=3$, $l=0$), it was found that a width of 3.5 kev provides a best fit compatible with the data and the other resonances. By subtracting this mutual-interference curve from the data, the wings of No. 12 are left sufficiently revealed to obtain its width of 4 kev for $J=4$ and $l=1$. The three *p*-wave peaks, Nos. 8, 10, and 11, then can be fitted by the following parameters: (*a*) For No. 10, $J=2$ and $\Gamma=3$ kev. (*b*) For Nos. 8 and 11, $J=1$ and $\Gamma=5$ and 3 kev, respectively. To account for the shapes of these last two resonances and to leave No. 10 as little distorted as possible, it was necessary to include their mutual interference. No way was found to account for the low-energy wing of No. 8 unless this interference was included. The high-energy wing of No. 11, which is left after subtracting the wings of Nos. 9 and 12, can also be better accounted for by the multiple-level computation than by single-level plots.

In the region between Nos. 12 and 19 the cross-section during early measurements appeared to be

unexplainably high, with a number of irregularities and small peaks in the curve. During the latest measurements with a neutron energy spread of about 350 ev, this region was re-studied. The results are shown in Fig. 3 where the variation in the cross section is sufficient to show the presence of a number of small resonances, Nos. 13 through 18, inclusive. This group of resonances is also shown in Fig. 13 after the wings of larger neighboring resonances, including the mutual interference of s-wave resonances, are subtracted off. The loci of the possible peak heights for $J=0$ and 1 are also shown in Fig. 13 and from these and the heights of the peaks in this group it appears that Nos. 13, 14 and 15 are attributable to $J=1$ and Nos. 15A, 16, 17, and 18 to $J=0$ ($l\geqslant 2$). From the high-energy wing of No. 18 and the low-energy wing of No. 13 one finds a width of 2 kev for each resonance. Single-level plots for Nos. 13 and 18 are also shown by dashed curves in Fig. 13. The residual curve obtained by subtracting the high-energy wing of No. 13 shows a peak No. 13A which is attributable to $J=1$ and has a width near 2 kev.

To continue the analysis it was found best to estimate the widths of Nos. 14 and 15 and compare the consequences with the data. After a number of adjustments it was found that a width of 2 kev for each of these two resonances for $l=1$ provides a best fit. Their wings are then compatible with the overlapping wings of other adjacent resonances. A better analysis of the various resonances is obtained by including the mutual interference of the wings of those p-wave resonances. This is particularly true for finding reasonable parameters for resonances Nos. 13B, 14A, and 15A. Except for the peak heights in the region of Nos. 13 to 15, the parameters shown in Table I for these ten resonances account very well for the data in this region.

(G) Analysis of the Resonances from 195 to 272 kev

Since the low-energy sides of the resonances show no pronounced minima and the high-energy wings have no apparent asymmetry, there does not appear to be an s-wave resonance present in this group (Fig. 4). However, the wings of the s-wave resonances Nos. 9, 31, and 38 in adjacent groups do extend into this region; but because of their remoteness, the cumulative mutual interference of the wings of these three resonances differs but little from the potential scattering, particularly over the lower half of this region. Their combined wings, which provide the background upon which the group sits, were first subtracted from the data.

Because of its larger width, it appears that No. 19 could be due to two or more peaks. However, during the latest measurements data points at 500-ev intervals with a neutron energy spread of approximately 350 ev failed to show the presence of more than one resonance. Its peak height exclusive of potential scattering is 5.7

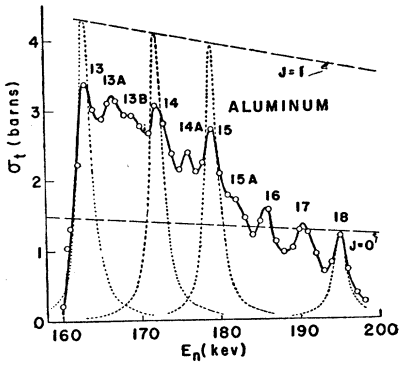

FIG. 13. Resonance structure of aluminum from 158 to 200 kev. The wings of the large neighboring resonances including the wings of s-wave resonances obtained by mutual interference calculations have been subtracted from the data leaving only the resonance scattering of the group of resonances shown here. The lines showing possible peak heights for $J=0$ and $J=1$ do not include the potential scattering.

barns (compared with possible heights of 3.5 and 5.8 barns for $J=1$ and 2, respectively) so the value of J is taken to be 2. On the assumption that this is a p-wave resonance, a width of 7 kev was obtained from the low-energy wing. The single-level plot fits this wing well and because of the very large width of this resonance, its wings extend an appreciable distance from the resonance. Hence, these wings were subtracted from all neighboring resonances before any further analyses were performed.

The peak height of No. 23 exclusive of potential scattering is 4.25 barns and by self detection 4.8 barns (shown by a cross in Fig. 4 before the wings of other resonances are subtracted) compared with possible values of 3.25 and 5.1 barns for $J=1$ and 2, respectively. Hence J is taken to be 2. The resonance appears to be symmetrical in shape and is, therefore, assumed to be due to a p-wave interaction. The wings are sufficiently revealed to obtain a width of 3 kev. The other three levels between Nos. 19 and 23 then peel off rather easily and yield the parameters shown in Table I. The mutual interference of Nos. 20 and 22 depresses the cross section by about 0.3 barn near the peak of No. 21. This aids in assigning a value of $J=2$ to No. 21.

The region from 225 to 272 kev is shown separately in Fig. 14. In the upper part of the figure are shown the data from the latest measurements for a neutron energy spread of about 350 ev. The points shown by crosses were obtained in a different run with a sample 0.6 as thick and a neutron energy spread of about 325 ev. In the lower part of the figure, curve A shows the results obtained when the wings of the s-wave resonances shown in Fig. 10 and the wings of Nos. 19, 23, and 28 are subtracted from the data. The fact that the cross section shown by curve A is not zero everywhere in the region shows that considerable level structure exists. The loci (exclusive of potential scattering) of the possible peak heights for $J=0$ and 1 are shown and indicate

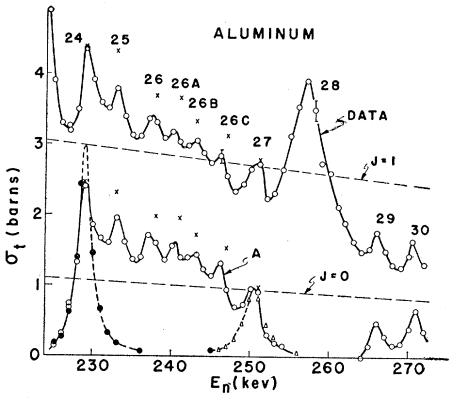

FIG. 14. Resonance structure of aluminum in the region from 225 to 272 kev. The wings of the 257-kev resonance No. 28 obtained by the single-level formula and those of the s-wave resonances obtained by the multiple-level formula have been subtracted from the data leaving in the lower part of this figure only the resonance scattering of the group shown here. Points represented by crosses were obtained with a neutron energy spread of 325 ev and a sample of aluminum 0.7 in. thick. The lines showing possible peak heights for $J=0$ and $J=1$ do not include the potential scattering.

that Nos. 27, 29, and 30 are attributable to $J=0$. The others appear to have a value of J no less than 1.

A single-level plot of No. 27 for a width of 3 kev is shown in Fig. 14 and appears to account for this peak. Also a single-level plot of No. 24 obtained by the parameters $J=1$, $l=1$, and $\Gamma=2$ kev is shown. For a value of $J=2$, No. 24 could hardly be attributed to a p-wave interaction, because mutual interference with No. 23 would then be expected to show a much deeper minimum between the two resonances. The spacing of 6 kev between the two levels is ample to observe such a minimum if it exists. One would expect the observed peak heights to be somewhat higher if any of the peaks Nos. 24 through 26C had a value of $J=2$. Measurements were made over this region on three different occasions and the highest peak cross sections obtained are shown in Fig. 14.

The set of parameters shown in Table I for this group was obtained as far as possible by the "peeling off" process and the two or three remaining resonances by trial and error. One can see from Fig. 14 that the average width could not be expected to be more than 2 kev. A multiple-level calculation then shows that the fully resolved minimum between Nos. 24 and 25 would be a little less than a barn (curve A).

(H) Analysis of the Group of Resonances from 272 to 355 kev

There are indications of s-wave resonances in this region (Figs. 5 and 6). The pronounced minimum of 1.35 barns at 272 kev on the low-energy side of resonance 31 would be expected to be even lower in the absence of the small peak No. 30. This minimum is very close to resonance No. 31 and, along with a rapid rise to the peak, identifies No. 31 as an s-wave resonance. The observed peak height is 5.6 barns compared with possible heights of 5.3 and 6.6 barns for $J=2$ and 3, respectively. Resonance No. 32 appears to be narrow and, with the high-energy wing of No. 31 as a background, it must have a relatively low peak and is, therefore, expected to contribute little to the peak of No. 31. The next s-wave resonance is apparently No. 38 and it is expected to depress the cross section in the region of No. 31 by about 0.5 barn. This amount added to the observed height of No. 31 indicates a value of $J=3$. From the low-energy wing one expects a width of about 5 kev.

The cross section is unusually large in the region above resonances Nos. 38 and 39 with no apparent group of peaks to account for it. To be sure that no additional detectable peaks exist in this region, further measurements were made. Although the measurements were repeated over the entire region with a neutron energy spread of about 350 ev, no resonance structure other than what is shown in Figs. 5 and 6 was observed. This region has the general asymmetrical shape of the high-energy wing of an s-wave resonance with the small peaks shown in Figs. 5 and 6 superimposed on it. The wings of the group of resonances Nos. 32 through 37 can contribute only slightly to the cross section in this region unless there be s-wave resonances present, and even then these could account for no more than a small fraction of the cross section. There does not then appear to be any way to account for this region except to take it to be the asymmetrical wing of a strong s-wave resonance together with possible interference with No. 31. It remains then to rule out either peak No. 38 or No. 39 as an s-wave resonance.

The observed peak heights of Nos. 38 and 39 uncorrected for contributions from other resonances are 5.7 and 4.9 barns, compared with possible single-level heights of 4.75 and 6 barns for $J=2$ and 3, respectively. Resonance No. 39 can be ruled out as an s-wave resonance by the following observations: (a) The width of No. 38 for any value of l appears to be 3 to 4 kev and consequently contributes so much to the peak height of No. 39 that the true peak height of No. 39 is much too low for even a value of $J=2$. (b) Even for a value of $J=2$ ($l=0$) for No. 39 (or No. 38), a further complication would arise. The mutual interference with No. 46 ($l=0$, $J=2$) would reduce the high-energy wing of Nos. 38 or 39 much more rapidly and reduce it below potential scattering (2 barns) in the region above 345 kev. Except for the small peak No. 42, contributions from other resonances are known to be small in this region. (c) Because of its height No. 39 would necessarily have a value of $J=2$ if due to s-wave interaction. (d) The low-energy wing of No. 38 appears to rise rapidly to its peak in a way similar to that of No. 31. Therefore, No. 38 is taken to be an s-wave resonance with $J=3$.

By use of the multiple-level formula, Eq. (2), assuming level widths from 3.5 to 5.5 kev, it was found

that the best set of parameters for the two s-wave levels is $E_r=278$ kev and $\Gamma=5$ kev for No. 31, and $E_r=311.8$ kev and $\Gamma=4$ kev for No. 38. After subtracting the multiple-level plot of these two resonances from the data, it was found that the remainder of the resonances in this region peel off rather easily and yield the parameters shown in Table I.

(I) Analysis of the Group of Resonances from 390 to 450 kev

All of the resonances of this group (Fig. 7) appear to be symmetrical in shape, with no pronounced dips on their low-energy sides. One, then, concludes that no s-wave resonances are present in the group. The high-energy wing of the s-wave resonance No. 46 does, however, extend into this region and provides a background upon which the group sits. This background is a little above the potential scattering (2 barns) and is first subtracted from the data. The remaining curve, then, represents only the resonance scattering of the various p and d wave resonances.

It is convenient to begin the analysis with resonance No. 54 because it is the widest one of the group and its wings are sufficiently well defined to obtain a reasonable width of 4 kev. The peak height is a few tenths of a barn below the possible value for $J=4$; and when the single-level plot of this resonance (obtained by the parameters $J=4$, $\Gamma=4$ kev and $l=1$) is subtracted from the data, the region is divided into two groups. The low-energy wing of No. 55 is then well defined so it can be peeled off. The next two, Nos. 56 and 57, also peel off readily. Because Nos. 57 and 58 were assigned common values of J and l, a multiple-level calculation was performed over the entire region of these two resonances. The result showed each resonance to be repelled by about 200 ev from the other and that there was an increase in peak height of each resonance by a few tenths of a barn and a small rise in the lower part of the extreme lower and upper wings of the two resonances. The depression between the two resonances is so narrow that one cannot observe the low minimum experimentally. The same effects were found for Nos. 55 and 56 as for Nos. 57 and 58.

Turning now to the resonances in the region below No. 54, one can begin the peeling-off process with No. 53 but it was found that, because of the relatively wide peak No. 50, less adjusting of the widths for a best fit was needed if the peeling-off is begun with No. 49. The parameters $J=3$, $\Gamma=2$ kev and $l=2$ account for No. 49. The peeling-off process then proceeds with a minimum of adjustments for a best fit. An adjustment was made to take into account the mutual interference of resonances Nos. 52 and 53.

The parameters shown in Table I for the dozen p- and d-wave resonances found in this region are the ones that were found to give a best over-all fit. The data indicate by the minimum above No. 58 that the next level is sevarel kev above this resonance and is not an s-wave resonance. One then concludes that the high-energy wing of No. 58 is little affected by the next unmeasured peak. The presence of another nearby s-wave resonance at higher energy would, because of its intereference with potential scattering (and a greater interference with No. 46 if $J=2$ for the s-wave resonance), depress the cross section in this region—particularly around Nos. 54 to 58. Should such an s-wave resonance exist, the spacing between it and No. 46 has to be at least 75 kev, and no drastic interference effects can be expected to occur to upset the value of J assigned to the various resonances of this group.

TABLE II. The number of levels and their distribution among the various values of the angular momentum J. The relative numbers are the ratios of the densities of levels to the density for $J=1$.

J	0	1	2	3	4
Number of levels	13	21	18	10	3
Relative numbers	0.61	1.00	0.86	0.48	0.14

A common value of $J=3$ is assigned to resonances Nos. 49, 50, and 51 and, if the same value of l is associated with all three resonances, deep interference minima should be observed between each pair of resonances, particularly between Nos. 49 and 50. This minimum is so wide that it could easily be resolved to a much lower depth if mutual interference of Nos. 49 and 50 is present. The absence of this deep minimum suggests a value of $l=2$ for Nos. 49 and 51 and a value of $l=1$ for No. 50, which is the widest of the three. The ratios of the Wigner limit of these three resonances to the reduced widths are 13.7, 7.6, and 19.3, respectively. The multiple-level plot for Nos. 52 and 53 shows a deep minimum between them but the wings of adjacent levels raise this minimum by a barn or more. This, along with a relatively narrow minimum, prevents one from observing a minimum much deeper than is shown. A common value of J and l for Nos. 52 and 53 cannot, therefore, be ruled out on this basis.

Table I shows a summary of the parameters of sixty-five of the sixty-six resonances determined from these analyses. Table II shows the number of levels assigned to each value of J (not including the one at 6 kev) and their distribution among the various values of J. This distribution and the values of Γ and l for the various resonances are only as valid as the analyses. The parameters are those that give a best fit to the data.

It is expected that the widths of resonances with high values of l should become progressively smaller (reference 16, page 464) with increasing l. However, there appear to be no really definite rules or characteristics that distinguish clearly between resonances with $l=1$ and 2. A comparison of the measured reduced width γ^2 with the Wigner limit, $\hbar^2/MR^2$ can be used as a rough guide.[19,20] From fairly well isolated resonances having

[19] C. E. Porter and R. G. Thomas, Phys. Rev. **104**, 483 (1956).
[20] R. G. Thomas, Phys. Rev. **97**, 224 (1955). See also S. E. Darden, Phys. Rev. **99**, 748 (1955). The latter used γ^2R for the

values of $J=0$ ($l\geqslant 2$), it was found that a d-wave resonance was indicated when the ratio of the Wigner limit to the measured reduced width was about 8 or larger. This finding was further strengthened in a number of cases in which $J>0$ and no deep minimum occured between a pair of resonances to indicate a common value of J and l for these pairs. The spacings are so great in many cases that these interference minima could have been detected easily if they were present. Therefore if the resonances of such a pair have the same J, they must differ in l. On this basis the levels are distributed approximately equally between the odd ($l=1$) and even ($l=0$ and 2) parities.

5. CROSS SECTION BELOW 30 KEV

Except in the region below 30 kev, the indications are that the potential scattering is about two barns, a value close to that given by $\sigma_p=\sum_l(2l+1)4\pi\lambda\!\!\!^{-2}\sin^2\delta_l$. The region below 30 kev is the largest one free of observed levels and one might at first expect to find the observed cross section here to be equal to the potential scattering cross section. However, throughout this region the cross section is consistently below the expected potential scattering. Moreover, although the shapes of the lower parts of the wings of the 35-kev resonance suffice to establish an s-wave interaction with certainty, they deviate somewhat from the usual shape for a single-level Breit-Wigner plot—particularly in the region around the minimum. Further, instead of the observed minimum of this resonance occurring at a rather definite energy close to the resonance and being followed by a rapid rise to the peak of the resonance, it is spread over a fairly large energy region and shifted to a lower energy than what is usually observed. This behavior of the cross section is presumed to be due to the cumulative mutual interference of the various s-wave resonances. According to Eq. (6), for a potential scattering of about 2 barns one would expect a minimum of about 1.2 barns for $J=2$ or 0.9 barn for $J=3$. The observed minimum of 0.5 ± 0.05 barn is lower than either of these expected values. The 0.9 barn attributable to $J=3$ will be unaffected by interference between a level ($J=3$) in the negative energy region and the 35-kev level if the latter has a value of $J=3$. The observed minimum of 0.5 barn, therefore, indicates that another resonance for which $J=2$ has a low-energy wing which extends into the region around 30 kev so that interference with the potential scattering lowers the cross section in this region. According to the present analyses, resonance No. 6 is attributed to an s-wave neutron interaction with $J=2$ and, because of its relatively wide width (4 kev), can account for the unexpectedly low minimum of the 35-kev resonance.

The mutual interference was computed by Eq. (2) for the various s-wave resonances having a value of $J=3$. These results are then combined with the potential scattering cross section and the low-energy wing of the s-wave resonance No. 6 ($J=2$) computed by Eq. (3) but do not quite account for the data. They do, however, show a cross section lower than the expected potential scattering and a shape similar to the observed shape of resonance No. 2. A level is also known to be present near -23 kev.[18] The mutual interference was recomputed by including this level, assumed to be an s-wave level with $J=3$ and $\Gamma=3$ kev. The results of these computations combined with the low-energy wing of No. 6 and the potential scattering are shown from 10 to 50 kev in Fig. 1, where the computed points are represented by the crosses. These points account for the low cross section below 30 kev and duplicate closely the observed shape of the wings of resonance No. 2. If the assumed width of the real level at -23 kev is altered to either 2.5 or 3.5 kev, a definitely poorer agreement with the data results.

These results also account for the deviations of the points from a straight line at low energies in Fig. 8 which shows the analysis of the 35-kev resonance. The observed cross sections in the region of the minimum are too low and those in the high-energy wing slightly too high for a single-level isolated resonance. Hence, since Y is too small when the cross section is too large and vice versa, the lines of Fig. 8 have too small a slope and thus indicate too small a value of the potential scattering. However, the widths determined by these lines are little affected by this because the principal effect of interference with other resonances was to cause a small clockwise rotation of the lines about some point near the center (peak) of the resonance.

6. DISTRIBUTION OF THE ANGULAR MOMENTA AMONG THE NUCLEAR LEVELS

The density of levels, as a function of the total angular momentum J, is given for the single-particle model by the expression[21]

$$\rho(U,J)=\rho(U)\{\exp[-J^2/2c\tau]-\exp[-(J+1)^2/2c\tau]\}, \quad (7)$$

where $c\tau$ is sometimes written as σ^2 by different authors, $\rho(U)$ is the density of all levels for the energy region in question, U is the excitation energy, τ is the so-called nuclear temperature that varies slowly with energy, and c is a constant having the value $(1/55)B^2A^{5/3}$ Mev^{-1} for

reduced width and consequently his strength functions are expressed in units of 10^{-13} cm. The expression $\bar{\Gamma}_n{}^0/D$, used for the strength function in low-energy neutron work, is subject to some error at higher energies because of an approximation made to obtain this form as discussed in reference 12. For a further discussion see reference 9 on page 484 of reference 19. The upper limit of γ^2 is approximately $\hbar^2/MR^2$ or $40/R^2$ Mev where R is in units of 10^{-13} cm. The upper limit for aluminum is then about 2.2 Mev.

[21] C. Bloch, Phys. Rev. **93**, 1094 (1954). See also H. A. Bethe, Revs. Modern Phys. **9**, 69 (1937), formula (301); J. M. B. Lang and K. J. LeCouteur, Proc. Phys. Soc. (London) **A67**, 586 (1954); T. D. Newton, Can. J. Phys. **34**, 804 (1956). The expression for $\rho(U,J)$ is written by various authors in the approximate form $\rho(U)[(2J+I)/2c\tau]\exp[-(J+\frac{1}{2})^2/2c\tau]$.

a nuclear radius given by $R=0.14A^{\frac{1}{3}}\times10^{-12}$ cm. Lang and LeConteur[21] found the constant B to have a value of 0.55 for a fit to observed level densities.

The number of levels of a single nuclide assigned experimentally to each different value of J hitherto has been too small to permit verification of the theoretical expression. In the present work a sufficient number of levels of aluminum have been identified with the various values of J to give a rough experimental check of the theoretical distribution. When Eq. (7) is used to compute the ratios of the densities of levels for different values of J to the density for $J=1$, the plots for $2c\tau=5$, 6, and 7 are as shown in Fig. 15. The experimental points for the relative numbers shown in Table II are also shown in the plot and a reasonably good fit is given for $2c\tau=6$. The constant c has a value of 1.4 Mev^{-1} so the corresponding value of τ is 2.1 Mev, which is reasonably close to the values indicated by the distributions of energy of neutrons emitted by various excited nuclei in the experiments discussed by Lang and LeCouteur.[21]

The foregoing analysis is based on the assumption that no great proportion of very narrow resonances of high J values have been missed. It is impossible to be perfectly sure on this point but the fit of the experimental points to a curve having the theoretical shape and the reasonable value of the quantity $c\tau$ required to obtain this fit suggest that no large number of such resonances have been missed.

The density of all levels for a particular excitation energy U is given by the summation

$$\sum_J \rho(U,J)=\rho(U), \tag{8}$$

where $\rho(U)$ is given by Bloch[21] in the form

$$\rho(U)=[\sigma U(96\pi)^{\frac{1}{2}}]^{-1}\exp[\pi(2U/3\delta)^{\frac{1}{2}}], \tag{9}$$

and δ was shown by Ross[22] to be given by

$$1/\delta=1/\delta_n+1/\delta_p. \tag{10}$$

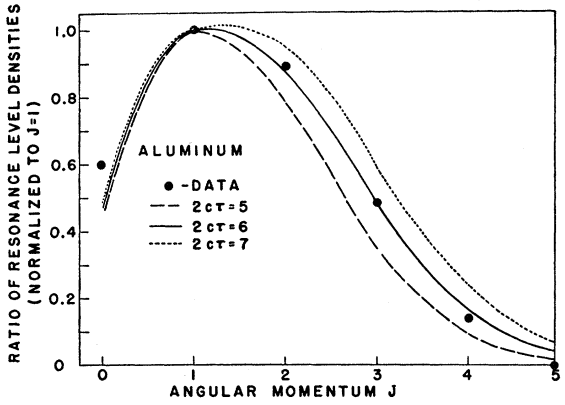

FIG. 15. Distribution of the angular momenta among the resonance levels of Al^{28}. Experimentally determined points are shown by solid circles. The curves are plots of Eq. (7) for values of $2c\tau=5$, 6, and 7.

[22] A. A. Ross, Phys. Rev. **108**, 720 (1957).

The quantity δ is the average level spacing of the individual nucleons in the nucleus, δ_n the spacing for neutrons and δ_p for protons.

From the present measurements the experimentally determined density of all levels is $\rho(U)=146$ Mev^{-1}. For a mean value of $U=7.95$ Mev and the value of $\sigma=1.73$ obtained from the distribution of the angular momenta, one obtains a value of $\delta=0.48$ Mev. Figure 1 of reference 22 gives a plot of the theoretical value of the average single-nucleon spacing δ. From this figure it appears that the theoretical value of δ for $A=28$ is about 0.45 Mev.

7. DISTRIBUTION IN THE SIZE OF THE NEUTRON WIDTHS

The reduced widths obtained from the neutron widths of the resonances by the relation[23] $\gamma^2=\Gamma_n/(2P_l)$ fluctuate rather violently among the levels of Al^{28}. Among various suggested theoretical expressions for these fluctuations, Porter and Thomas[19] expect the distribution $x^{-\frac{1}{2}}\exp(-X/2)$ to be more reasonable on theoretical grounds. The quantity $X=\gamma^2/(\gamma^2)_{\text{Av}}$ is evaluated for a given J and l, where $(\gamma^2)_{\text{Av}}$ is the average for the particular J and l. In studies made by Hughes and Harvey[24] at low energies for intermediate and heavy nuclei, they find reasonable agreement with the Porter-Thomas distribution but do not rule out the exponential distribution. For convenience the Porter-Thomas distribution can be given in the form

$$y=CX^{-\frac{1}{2}}\exp(-X/2),$$

or

$$\ln(X^{\frac{1}{2}}y)=-X/2+\ln C, \tag{11}$$

where C is a constant which depends on the number of levels and y is the number of levels per interval ΔX. In addition to the Porter-Thomas distribution, a number of others (such as the exponential, the Bethe, and other distributions) have been compared with the present data. Figure 16 (a) shows ΔX, the number of levels per interval, plotted as a function of X for the present data. The straight line shown in the figure is an exponential plot for an arbitrarily chosen value $C=33$. This distribution appears to agree with the data. However, the Porter-Thomas distribution shown in Fig. 16 (b) is also in fair agreement with the data and is a better fit to the data than the Bethe distribution $X^{-\frac{1}{2}}\exp(-X^{\frac{1}{2}})$ shown in Fig. 16 (c). Plots of the distributions $\exp(-X^2/2)$ and $X\exp(-X^2)$ yield curves instead of straight lines and do not agree with the data. The points represented by crosses in Fig. 16 show the effect of including the narrow level at 6 kev with the assumed parameters $J=2$, $l=0$, and $\Gamma=10$ ev.

Although the plots shown in Fig. 16 do not decide

[23] The penetrability factors P_l are given by $kR\nu_l$ and the ν_l are given in reference 16, p. 361.

[24] D. J. Hughes and J. A. Harvey, Phys. Rev. **99**, 1032 (1955), and **109**, 471 (1958).

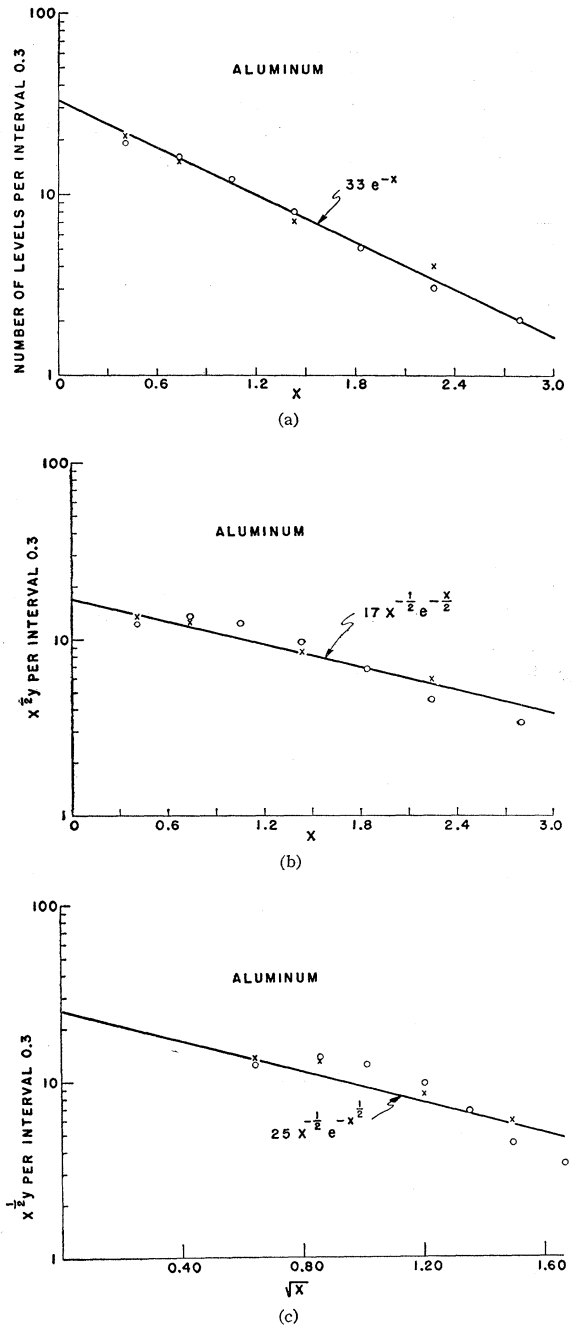

FIG. 16. Distribution (per 0.3 in ΔX) in the size of the reduced neutron widths of Al^{28}. (a) Exponential distribution, (b) Porter-Thomas distribution, and (c) Bethe distribution. See text for an explanation of points represented by crosses.

definitely in favor of any one of the three distributions, they do tend to favor the exponential distribution. As a further check, the percentages of resonances with widths smaller than a particular value of X have also been plotted and compared with plots of the integral $\int_0^x e^{-X}$ for the exponential distribution and the integral $\int_0^x X^{-\frac{1}{2}}e^{-X/2}dX$ for the Porter-Thomas distribution. It was found that the exponential distribution lies between the data and the Porter-Thomas distribution for small values of X but each distribution approaches the experimental points as X increases and practically coincides with them for the largest values of X. Thus both distributions indicate either that a few more narrow levels should have been observed or that the observed widths of the narrow levels are too large. Four to six additional narrower levels could lead to a very good agreement with the exponential distribution but a larger number would be necessary for an agreement with the Porter-Thomas distribution.

8. DISTRIBUTION OF THE LEVEL SPACINGS

Some attempts have been made to discover the law which governs the distribution of spacings of adjacent energy levels of the same spin and parity.[25] The assumption has also been made that one would expect the probability of a certain spacing to be an exponential function of the spacing. For convenience this can be expressed in the form

$$N=c\exp(-\mathcal{S}), \tag{12}$$

where $\mathcal{S}=S/D$. The quantity S represents the level spacing and D the average level spacing for a given J and parity. The quantity c is a constant and N is the number of level spacings per interval $\Delta\mathcal{S}$. The number of level spacings per interval $\Delta\mathcal{S}$ is plotted as a function of $\mathcal{S}$ in Fig. 17 for the present data. For comparison, the exponential distribution for a value of $c=28$ is also shown. The exponential distribution appears to agree with the data.

Recently Wigner[25] proposed the distribution

$$N=c\pi(\mathcal{S}/2)\exp(-\pi\mathcal{S}^2/4) \tag{13}$$

on the basis that, at least for small values of S for zero-spin nuclei, the probability of finding a level in an interval dS is proportional to $(S\,dS/D)$. If this probability should also hold for large values of S, Eq. (13) could be used for all values of S and for convenience is expressed in the form

$$\ln(N\mathcal{S}^{-1})=-(\pi\mathcal{S}^2/4)+\ln(c\pi/2). \tag{14}$$

Since the various values of $\mathcal{S}$ for the present data are computed for a given J and parity, $\mathcal{S}$ should not depend

[25] Fujimoto, Fukuzawa, and Oaki, Progr. Theoret. Phys. (Kyoto) **16**, 246 (1956); I. I. Gurevich and M. I. Pevsner, J. Exptl. Theoret. Phys. U.S.S.R. **31**, 162 (1956) [translation: Soviet Phys. JETP **4**, 278 (1957)]; Nuclear Phys. **2**, 575 (1956/57); E. P. Wigner, Proceedings of the Conference on Neutron Physics by Time-of-Flight, Gatlinburg, Tenn., 1956 [Oak Ridge National Laboratory Report ORNL-2309 (unpublished)]; E. P. Wigner, Proceedings of International Conference on Neutron Interactions with Nuclei, Columbia University, 1957 [Atomic Energy Commission Report TID-7547 (unpublished)]; L. Landau and Y. Smorodinsky, *Lectures on Nuclear Theory* (English translation) (Consultants Bureau, Inc., 227 West 17th Street, New York), see second paragraph at top of p. 55; N. Rosenzweig, Phys. Rev. Lett. **1**, 24 (1958); S. Blumberg and C. E. Porter, Phys. Rev. **110**, 786 (1958). See also J. A. Harvey and D. J. Hughes, Phys. Rev. **109**, 471 (1958).

on the spin of the target nucleus. However, a plot of $\ln(N\mathcal{S}^{-1})$ *vs* $\mathcal{S}^2$ for the present data yields a curve instead of a straight line and does not agree with the data.

The percentages of spacing smaller than a particular value of $\mathcal{S}$ have been plotted also and compared with a plot of the integral $\int_0^{\mathcal{S}} \exp(-\mathcal{S})d\mathcal{S}$. The data follow the general trend of the exponential distribution except for a small hump near the middle of the curve. The entire curve for the integral $(\pi/2)\int_0^{\mathcal{S}} \mathcal{S}\exp(-\pi\mathcal{S}^2/4)d\mathcal{S}$ falls far below the data. A plot of the data was also made in which the various values of $\mathcal{S}$ were computed without regard to J and parity. This plot does not agree with either of the foregoing distributions.

9. STRENGTH FUNCTIONS

The strength function is $(\gamma^2)_{Av}/D$, the average ratio[20] of reduced width to spacing, where the reduced width[23] $\gamma^2=\Gamma_n/(2P_l)$ and D are averaged for a given value of l. Averaged over both values of J for the s-wave resonances in the present measurements, the strength function is 0.05; and averaged over all values of J for the p-wave resonances it is 0.49, which is approximately ten times as large as for s-wave resonances. These results are in accord with the complex square-well model of Feshbach, Porter, and Weisskopf[15] who, for a nuclear well depth of 40 Mev, predict a p-wave maximum near $A=27$ and a low value for s-wave resonances. The sum rule of Lane, Thomas, and Wigner[26] suggests that the sum of the reduced widths of a given group of resonances in an energy interval comparable with the spacings of giant resonances for a given value of l should not exceed $\hbar^2/MR^2$. For the p-wave resonances in the present measurements, this sum is 0.35 of the Wigner limit and indicates that this interval of energy is near the maximum for the strength function for $l=1$. The strength function calculated for the d-wave resonances found here appears to be too high in comparison with the p-wave strength function. This could be the result of having assigned too many resonances to a value of $l=2$. This possible error would have little effect on the p-wave strength function because a calculated value for the latter is only a little more than 0.6 even if all resonances in question are interpreted as p-wave resonances. Because of the nuclear shell effects, it is conceivable that the expression for P_2 is incorrect and could cause a large value of the strength function for the d-wave resonances.

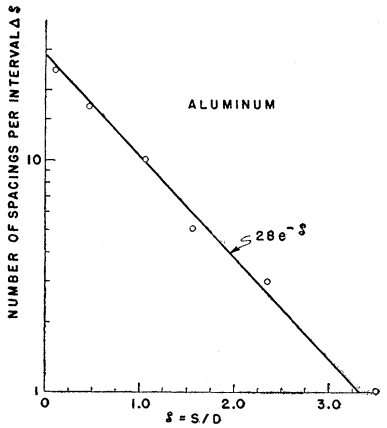

FIG. 17. Distribution of the level spacings of Al^{28}.

10. DISCUSSION

The results have shown the feasibility of resolving the complicated level structure of a nuclide to such an extent that reasonable values of the angular momentum J can be determined. Initial measurements with neutron energy spreads ranging between 400 and 700 ev revealed the presence of many resonances. It was thought that the distribution of the values of J among the resonances might possibly show a larger fraction of the higher values of J. Several recent experiments with neutron energy spreads ranging from 300 to 400 ev have failed to do more than increase some of the peak heights by small amounts and lower some minima between peaks by small amounts. The results of the recent experiments are shown in the various figures and show the highest peak values obtained. Although one might expect to resolve some of the peaks to somewhat higher values by even smaller neutron widths, it is not expected that any drastic changes would occur in view of the observed widths of the levels. The degree to which resonances of different widths are resolved appears to agree with measurements on other elements for which the level spacings are greater.

The quantitative estimates of the components of low-energy neutrons in beams of three different energies are in agreement with previous measurements. (See the last paragraph of Sec. 3 and reference 12 for a discussion and references to original papers.)

It is expected that any errors which may have occured in evaluating the widths of resonances would tend toward values that are too wide, particularly for the narrow resonances. There are two indications of this. A high value of the strength function for the d-wave resonances might be due in part to this and in part to assigning too many resonances to a value of $l=2$. The size distribution of the neutron widths, although apparently in agreement with the exponential distribution and less well with the Porter-Thomas distribution, would be in even better agreement if the narrow resonances should show a trend toward somewhat narrower widths.

In view of the limited number of observed levels and the limitations of the analyses in consequence of the difficulties in resolving the narrow levels to heights nearer their true peak heights, the conclusions drawn from the results can be expected to be somewhat tentative. In particular it appears that a tremendous number of levels for many isotopes will be needed to definitely decide between the exponential and the Porter-Thomas distribution for the size distribution of the neutron widths. Further developments in the theory

[26] Lane, Thomas, and Wigner, Phys. Rev. **98**, 693 (1955).

and the observation of many more level spacings are expected to lead to a better understanding of the level spacings.

It has been pointed out by Sailor[27] that for s-wave neutron resonances the compound nucleus appears to be formed preferentially by the spin state $J=I+\frac{1}{2}$ rather than by an even distribution between the states $J=I+\frac{1}{2}$ and $I-\frac{1}{2}$. The present results tend to agree with this observation. Five of the seven s-wave resonances were assigned to the spin state $J=I+\frac{1}{2}$ and the level at -23 kev appears to be an s-wave level having this same value of the spin.

Finally, it was found after offering an explanation for the low cross section in the region below 30 kev that the potential scattering cross section of this nucleus is very closely given by the expression

$$\sigma_p=\sum_l(2l+1)4\pi\lambda^2\sin^2\delta_l,$$

and one could have proceeded just as well with the analyses by tacitly assuming this value of the potential scattering cross section.

[27] V. L. Sailor, Phys. Rev. **104**, 736 (1956).

ACKNOWLEDGMENTS

In conclusion, I wish to express my appreciation to Dr. L. A. Turner for his suggestions and criticisms, to Dr. F. E. Throw for his comments and suggestions with the manuscript, to Dr. Norbert Rosenzweig and Dr. J. E. Monahan for their discussions concerning the distributions of the angular momenta, the level spacings and the neutron widths, to Dr. J. P. Schiffer for his discussions concerning the strength functions and size distribution of the neutron widths, to Jack Wallace for his aid in operating the Van de Graaff generator, and to the Van de Graaff crew consisting of Walter Ray, Jr., William Evans, Ronald Amrein, Robert Kickert, John Bicek, Edward Saller, and Robert Petersen.

PHYSICAL REVIEW VOLUME 114, NUMBER 1 APRIL 1, 1959

Differential Elastic Scattering of Neutrons from Neon

H. O. COHN AND J. L. FOWLER
Oak Ridge National Laboratory, Oak Ridge, Tennessee
(Received November 12, 1958)

Neutron elastic scattering from neon of natural abundance has been investigated in the energy range 0.8 to 1.9 Mev. The total cross section was measured by the standard method of attenuating a neutron beam by a sample, which in this case was neon gas contained in a meter-long steel cylinder at high pressure. Differential cross sections were observed both by measuring neon recoil energies in a proportional counter and also by detecting neutrons with an anthracene crystal in coincidence with neon recoils. The combination of techniques shows up resonances at the following energies (in Mev) with spin and parity assignments given in parentheses: 0.91 ($\frac{3}{2}-$); 1.28 ($\frac{3}{2}-$); 1.31 ($\frac{1}{2}-$); 1.37 ($\frac{3}{2}$ or $\frac{5}{2}+$); 1.62 ($\frac{3}{2}-$); 1.68 ($\frac{3}{2}+$); and 1.85 ($\cdots$). These resonances have reduced widths of the order of one percent of the Wigner limits.

INTRODUCTION

ELASTIC scattering of neutrons from zero-spin nuclei is of special interest. Since, in such cases as the scattering of neutrons from He^4,[1–3] C^{12},[4–11] O^{16},[12–15] and Ne^{20},[16–18] there is only one channel spin state, a unique phase-shift analysis of differential scattering data is possible, at least at low energies. Phase shifts so obtained in the case of He^4 neutron scattering,[3] and also in the case of O^{16},[14] can be discussed in terms of a single-particle picture, for in these cases one is dealing with the interaction of a neutron with closed-shell nuclei. This type of analysis seems to hold approximately even for neutron scattering from C^{12}.[11] It is of some interest, then, to investigate neutron scattering from Ne^{20} which is a nucleus rather far removed from a closed shell. Such an investigation, of course, leads to detailed knowledge of virtual states of Ne^{21}. Furthermore, a phase-shift analysis of neutron scattering from light zero-spin nuclei furnishes one a tool to measure the polarization of neutron sources.[4–6,11,15,19–23]

[1] P. Huber and E. Baldinger, Helv. Phys. Acta **25**, 435 (1952).
[2] J. D. Seagrave, Phys. Rev. **92**, 1222 (1953).
[3] E. Van der Spuy, Nuclear Phys. **1**, 381 (1956).
[4] R. Ricamo, Nuovo cimento **10**, 1607 (1953).
[5] Meier, Scherrer, and Trumpy, Helv. Phys. Acta **27**, 577 (1954).
[6] R. Budde and P. Huber, Helv. Phys. Acta **28**, 49 (1955).
[7] Little, Leonard, Prud'Homme, and Vincent, Phys. Rev. **98**, 634 (1955).
[8] Willard, Bair, and Kington, Phys. Rev. **98**, 669 (1955).
[9] M. Walt and J. R. Beyster, Phys. Rev. **98**, 677 (1955).
[10] Muehlhause, Bloom, Wegner, and Glasoe, Phys. Rev. **103**, 720 (1956).
[11] Wills, Bair, Cohn, and Willard, Phys. Rev. **109**, 891 (1958).
[12] R. K. Adair, Phys. Rev. **92**, 1491 (1953).
[13] A. Okazaki, Phys. Rev. **99**, 55 (1955).
[14] J. L. Fowler and H. O. Cohn, Phys. Rev. **109**, 89 (1958).
[15] Striebel, Darden, and Haeberli, Nuclear Phys. **6**, 188 (1958).
[16] H. O. Cohn and J. L. Fowler, Phys. Rev. **99**, 1625 (1955).
[17] H. O. Cohn and J. L. Fowler, Bull. Am. Phys. Soc. Ser. II, **1**, 175 (1956).
[18] C. P. Sikkema, Nuclear Phys. **3**, 375 (1957).
[19] E. Baumgartner and P. Huber, Helv. Phys. Acta **26**, 545 (1953).
[20] Adair, Darden, and Fields, Phys. Rev. **96**, 503 (1954).
[21] Willard, Bair, and Kington, Phys. Rev. **95**, 1359 (1954).
[22] Levintov, Miller, and Shamshev, Nuclear Phys. **3**, 221 (1957).
[23] Levintov, Miller, Tarumov, and Shamshev, Nuclear Phys. **3**, 237 (1957).